Vol. 81, No. 23

7SL RNA Mediates Virion Packaging of the Antiviral Cytidine Deaminase APOBEC3G[▽]

Tao Wang,[1]† Chunjuan Tian,[1,3]† Wenyan Zhang,[1,3]† Kun Luo,[1] Phuong Thi Nguyen Sarkis,[1] Lillian Yu,[1] Bindong Liu,[1] Yunkai Yu,[1] and Xiao-Fang Yu[1,2]*

Department of Molecular Microbiology and Immunology, Johns Hopkins Bloomberg School of Public Health, Baltimore, Maryland 21205[1]; Second Affiliated Hospital, School of Medicine, Zhejiang University, Zhejiang, China[2]; and Jilin University, Changchun, China[3]

Cytidine deaminase APOBEC3G (A3G) has broad antiviral activity against diverse retroviruses and/or retrotransposons, and its antiviral functions are believed to rely on its encapsidation into virions in an RNA-dependent fashion. However, the cofactors of A3G virion packaging have not yet been identified. We demonstrate here that A3G selectively interacts with certain polymerase III (Pol III)-derived RNAs, including Y3 and 7SL RNAs. Among A3G-binding Pol III-derived RNAs, 7SL RNA was preferentially packaged into human immunodeficiency virus type 1 (HIV-1) particles. Efficient packaging of 7SL RNA, as well as A3G, was mediated by the RNA-binding nucleocapsid domain of HIV-1 Gag. A3G mutants that had reduced 7SL RNA binding but maintained wild-type levels of mRNA and tRNA binding were packaged poorly and had impaired antiviral activity. Reducing 7SL RNA packaging by overexpression of SRP19 proteins inhibited 7SL RNA and A3G virion packaging and impaired its antiviral function. Thus, 7SL RNA that is encapsidated into diverse retroviruses is a key cofactor of the antiviral A3G. This selective interaction of A3G with certain Pol III-derived RNAs raises the question of whether A3G and its cofactors may have as-yet-unidentified cellular functions.

Human cytidine deaminase apolipoprotein B mRNA-editing catalytic polypeptide-like 3G (APOBEC3G [A3G]) and other APOBEC3 proteins (25) are related to a family of proteins that also includes apolipoprotein B-editing catalytic subunit 1 (APOBEC1), APOBEC2, and activation-induced cytidine deaminase (AID) (23, 66). These proteins have cytidine deaminase activities that modify RNA or DNA. A3G was the first APOBEC3 protein to be identified as a potent inhibitor of HIV-1 in the absence of Vif (59). A major outcome of virion packaging of A3G is the induction of C-to-U mutations in the minus-strand viral DNA during reverse transcription (22, 32, 42, 43, 63, 73, 77). Virion-packaged A3G and A3F can also reduce the accumulation of viral DNA (3, 21, 27, 40, 45, 57, 71) and the formation of proviral DNA (40, 45). Subsequently, several other human APOBEC3 proteins, including APOBEC3F (4, 35, 68, 79), APOBEC3B (4, 14, 72), APOBEC3A, and APOBEC3C (31, 72), have been identified as broad antiviral factors against human immunodeficiency virus type 1 (HIV-1), simian immunodeficiency viruses (SIV), murine leukemia virus, and hepatitis B virus (65), as well as endogenous retroelements (5, 6, 10, 17, 19, 50, 58, 61).

In order to successfully replicate in their hosts, retroviruses have developed multiple strategies for evading the antiviral functions of cytidine deaminases. Lentiviruses such as HIV-1 and SIV encode the Vif protein, which induces polyubiquiti-

nation and degradation of multiple APOBEC3 molecules (13, 37, 38, 44, 46, 60, 62, 74). Vif molecules of HIV-1 and SIV are newly identified substrate receptor proteins that assemble with Cul5, ElonginB, ElonginC, and Rbx1 to form an E3 ubiquitin ligase (29, 37, 41, 46, 74, 75). The most conserved motif among all lentiviral Vif proteins, SLQxLA, is a virus-specific BC-box motif that mediates the interaction with ElonginC (46, 74, 75), which in turn interacts with ElonginB and Cul5. To selectively bind Cul5, primate lentiviral Vif molecules use another highly conserved $Hx_5Cx_{17-18}Cx_{3-5}H$ motif (41). This motif binds zinc and stabilizes a highly conserved hydrophobic interface in Vif that mediates Cul5 selection (41, 47, 69, 70).

In the absence of the Vif protein, A3G can be packaged into diverse retroviruses and mediates potent antiviral functions in newly infected target cells. Encapsidation of A3G into HIV-1 particles is mediated by the Gag molecules (1, 9, 15, 39, 51, 56, 76). Most studies have found that the RNA-binding nucleocapsid (NC) domain of Gag molecules is required for efficient A3G packaging (1, 9, 15, 39, 51, 56, 76). Some groups have observed that the interaction between HIV-1 Gag and A3G is resistant to RNase treatment (1, 9). Other groups have reported that the interaction between HIV-1 Gag and A3G requires RNA (8, 56, 64, 76), suggesting a role for RNA in mediating A3G packaging. While two studies have reported that viral genomic RNA is required for efficient A3G packaging (28, 64), many studies have found that viral genomic RNA is dispensable (1, 9, 15, 28, 39, 51, 56, 64, 76), suggesting a role for cellular RNA in the virion packaging of A3G. Viral Pol proteins that are required for packaging of tRNAs into HIV-1 virions are also dispensable for A3G packaging (1, 9, 15, 28, 39, 51, 56, 64, 76). Thus, the cellular factors (RNAs) that interact with A3G and mediate its virion packaging remain to be iden-

tified. Interactions of A3G with Y RNAs, Alu RNAs, and various mRNAs have been reported recently (12, 20, 30). However, the role of these RNAs in mediating A3G packaging into HIV-1 virions is unclear.

In the present study, we demonstrate that A3G selectively interacts with 7SL RNA and certain Y RNAs in virus-producing cells. However, 7SL RNA, but not Y RNAs, is selectively packaged into HIV-1 virions. A similar virion packaging mechanism is used by A3G and 7SL RNA. Inhibiting 7SL RNA packaging into HIV-1 virions also impairs A3G packaging and its antiviral function. Since 7SL RNA has been detected in diverse retroviruses, the findings reported here provide a possible solution to the mystery of how A3G is capable of targeting diverse retroviruses.

MATERIALS AND METHODS

Plasmid construction. Infectious molecular clones of the parental wild-type HIV-1pNL4-3 and Vif mutant (pNL4-3ΔVif) constructs were obtained from the AIDS Research Reagents Program, Division of AIDS, National Institutes of Allergy and Infectious Diseases (NIAID), National Institutes of Health. The HIV-1 constructs BH10.FS−.Vif− (NC positive) and ZWT-p6.Vif− (NC replaced by a yeast leucine zipper domain) were described previously (9). The A3G-HA expression vector has been described previously (74). The SRP19 was amplified by reverse transcription-PCR (RT-PCR) using mRNA from H9 cells with the forward primer 5′-GTACGCGGCCGCATGGCTTGCACTGCCGC and the reverse primer 5′-GAGAGGGAAGTAAAAAAGGGAAAGGAAAG AAAAAGAAGGAACAAAAACTCATATCAGAAGAAGATCTTTAAGGA TCCATCG containing NotI and BamHI sites, respectively, and a C-terminal c-*myc* tag. The PCR product was cloned into VR1012 to generate SRP19-Myc. SRP19Δ6 was created from SRP19-Myc by deleting the coding sequences for amino acids 8 to 13 in SRP19, which have been shown to bind 7SL RNA (54). The 7SL RNA expression vector was constructed as previously described (49). Human 7SL cDNA was amplified from cDNA (made from RNA isolated from 293T cells) by using a BglII site-anchored forward primer (5′-GGAGATCTGC CGGGCGCGGTGGCGCGTGC-3′) and a HindIII site-anchored reverse primer (5′-GGAAGCTTAGAGACGGGGTCTCGCTATG-3′). The sequence-verified, amplified cDNA was digested with BglII/HindIII and cloned behind the H1 RNA promoter in plasmid pSUPER (OligoEngine) at the BglII/HindIII sites to obtain plasmid pSUPER-7SL. BH10(FS) and Zwtp6 were gifts from Shan Cen.

Antibodies and cell culture. The following antibodies were used for the present study: anti-p24 monoclonal antibody (MAb; AIDS Research and Reference Reagents Program, Division of AIDS, NIAID, National Institutes of Health, catalog no. 1513), anti-A3G antibody (AIDS Research and Reference Reagents Program, Division of AIDS, NIAID, National Institutes of Health, catalog number 9968), mouse anti-hemagglutinin (anti-HA) MAb (Covance, catalog no. MMS-101R-1000), anti-La (BD Transduction Laboratories, catalog no. 610905), anti-Ro60 (PROGEN Biotechnik, catalog no. 57040), anti-SRP54 (BD Biosciences), and anti-human ribosomal P antigen (Immunovision, catalog no. HP0-0100) antibodies. The bivalent anti-CD3/8 antibody was a gift of Johnson Wong (Massachusetts General Hospital, Boston, MA). 293, 293/A3G-HA, and 293T cells were maintained in Dulbecco modified Eagle medium (DMEM; Invitrogen) with 10% fetal bovine serum and penicillin-streptomycin (D-10 medium) and passaged upon confluence. Jurkat, Jurkat/A3G-HA, and CD4⁺ cells were maintained in RPMI 1640 medium (Invitrogen) supplemented with 10% fetal bovine serum with penicillin-streptomycin (R-10 medium).

Transfections, virus and VLP purification, and virion-associated RNA extraction. DNA transfection was carried out by using Lipofectamine 2000 (Invitrogen) as recommended by the manufacturer. Viruses in cell culture supernatants were cleared of cellular debris by centrifugation at 3,000 rpm for 15 min in a Sorvall RT 6000B centrifuge and filtration through a 0.2-μm-pore-size membrane (Millipore). Virus particles were then concentrated by centrifugation through a 20% sucrose cushion by ultracentrifugation at $100,000 \times g$ for 2 h at 4°C in a Sorvall Ultra80 ultracentrifuge. Viral pellets were resuspended in lysis buffer (phosphate-buffered saline [PBS] containing 1% Triton X-100, Complete protease inhibitor cocktail [Roche], and RNase inhibitor [New England Biolabs]). Viral lysates were analyzed by immunoblotting, or virion-associated RNA was extracted with TRIzol (Invitrogen) according to the manufacturer's instructions.

Immunoblot analysis. Cells were collected at 48 h after transfection. Cell lysates and viral lysates were prepared as previously described (74). Samples were lysed in 1× loading buffer (0.08 M Tris [pH 6.8], with 2.0% sodium dodecyl sulfate [SDS], 10% glycerol, 0.1 M dithiothreitol, and 0.2% bromophenol blue) and boiled for 5 min, and proteins were separated by SDS-polyacrylamide gel electrophoresis (PAGE). Membranes were probed with various primary antibodies against proteins of interest. Secondary antibodies were alkaline phosphatase-conjugated anti-human, anti-rabbit, or anti-mouse (Jackson Immunoresearch, Inc.) antibodies, and staining was carried out with BCIP (5-bromo-4-chloro-3-indolylphosphate) and nitroblue tetrazolium solutions prepared from chemicals obtained from Sigma. Blots were imaged by using a FujiFilm LAS-1000 Image Station, and protein band densities were analyzed by using the spot density analysis software Image Gauge V3.41. The percent decrease in A3G packaging levels was analyzed after normalizing the p24 antigen content, as determined by immunoblotting. Values for the positive control (no SRP19) were set to 100%, and the relative packaging of SRP protein-transfected samples was calculated as a fraction of the positive control.

Immunoprecipitation. To identify A3G-binding proteins, 293/A3G-HA cells were harvested, washed twice with cold PBS, and then lysed with lysis buffer (PBS containing 1% Triton X-100, Complete protease inhibitor cocktail [Roche], and RNase inhibitor [New England Biolabs]) at 4°C for 30 min. Cell lysates were clarified by centrifugation at $10,000 \times g$ for 30 min at 4°C. Anti-HA agarose beads (Roche, catalog no. 190-119) were mixed with the precleared cell lysates and incubated at 4°C for 3 h on an end-over-end rocker. The reaction mixtures were then washed six times with cold lysis buffer and eluted with 0.1 M glycine-HCl buffer (pH 2.0), followed by SDS-PAGE. The gel was fixed in a 50% methanol–10% acetic acid mixture for 10 min, stained with mass spectrometry-compatible colloidal Coomassie brilliant blue G-250 (Bio-Rad, catalog no. 1610406) staining solution (20% methanol, 8% ammonium sulfate, 1.6% phosphoric acid, 0.08% Coomassie blue G-250) to detect protein bands, and destained with distilled water. Protein standard markers (Bio-Rad, catalog no. 1610314) were used for estimating protein size. Protein bands of interest were cut out of the gel and rinsed twice with 50% methanol (high-pressure liquid chromatography grade). In-gel digestion was performed on protein bands cut out of colloidal Coomassie blue-stained SDS-polyacrylamide gels using sequencing-grade modified trypsin (Promega). Extracted peptides were cocrystallized in 2,5-dihydroxybenozic acid or αcyano-4-hydroxycinnamic acid (10 mg/ml in 50% acetonitrile–0.3% trifluoroacetic acid) and analyzed by matrix-assisted laser desorption ionization time-of-flight spectrometry on a Voyager DE STR (Applied Biosystems) using the Voyager instrument control panel (v 5.1) and Data Explorer (v4.0). The data were acquired in reflector mode, and masses were externally calibrated by using a standard peptide mixture to better than 50 ppm error. Proteins were identified by searching the acquired monoisotopic masses against the National Center for Biotechnology Information nonredundant or SwissProt databases using the MS-Fit search engine of ProteinProspector (prospector.ucsf.edu).

Analysis of virus infectivity. Virus infectivity was assessed with the MAGI cell line. MAGI-CCR-5 cells were prepared in 12-well plates in D-10 medium 1 day before infection, and the cells were at 30 to 40% confluence on the day of infection. Supernatants from transfected 293T cell cultures were clarified by low-speed centrifugation ($1,000 \times g$, 10 min) and then filtered through 0.22-μm-pore-size sterile filters. The culture medium was removed from each well, and serial 10-fold dilutions of virus, in a total volume of 200 μl of complete DMEM with 20 μg of DEAE-dextran/ml, were added to the monolayer cultures of MAGI cells, followed by incubation at 37°C. After 2 h, 1 ml of complete DMEM was added to each well, and 48 h later the cells were fixed with fix solution (PBS containing 1% formaldehyde and 0.2% glutaraldehyde), washed with PBS, and incubated for 2 h at 37°C with staining solution (20 μl of 0.2 M potassium ferrocyanide, 20 μl of 0.2 M potassium ferricyanide, 2 μl of 1 M MgCl₂, and 10 μl of 40 mg of X-Gal [5-bromo-4-chloro-3-indolyl-β-D-galactopyranoside]). Staining was stopped by removing the staining solution, and the cells were washed twice with PBS. Blue-stained cells (nuclei) were counted by using a light microscope, and viral infectivity was determined after normalizing the amount of input virus in terms of the p24 antigen content.

Quantitative real-time PCR (qRT-PCR). (i) Sample preparation. RNA samples were obtained from cell lysates or immunoprecipitated samples and treated with DNase by incubation in 10 μl of diethyl pyrocarbonate-treated water with 1× RQ1 RNase-Free DNase buffer, l μl of RQ1 RNase-free DNase (Promega), and 4 U of RNase inhibitor (New England Biolabs) for 30 min at 37°C. DNase was inactivated by the addition of 1 μl of RQ1 DNase stop solution and incubated at 65°C for 10 min. RNA was reverse transcribed by using random primers and the Multiscribe reverse transcriptase from the high-capacity cDNA archive kit (Applied Biosystems) according to the manufacturer's instructions. The

cDNA was either undiluted or serially diluted in diethyl pyrocarbonate-treated water before input into the real-time reaction to ensure that the amplification was within the linear range of detection. For the immunoprecipitation of endogenous A3G, 10 μg of bivalent anti-CD3/8 antibody (Johnson Wong) was added to 2×10^6 freshly isolated peripheral blood mononuclear cells in 10 ml of R-10 medium with 10 IU of interleukin-2 (IL-2; Roche)/ml. This bivalent antibody depletes CD8 cells and stimulates the outgrowth of CD4 cells from the culture. An additional 10 ml of R-10 medium containing IL-2 (10 IU/ml) was added after 2 days. After 5 days in culture, immunoprecipitation of A3G was performed, and RNA was isolated from coprecipitated samples as described above.

qRT-PCR reagents and conditions. The ABI 7000 sequence detection system (Applied Biosystems) was used for RT-PCR amplifications. All primers were synthesized by Invitrogen, and fluorescence-tagged probes were synthesized by Applied Biosystems. Agarose gel analysis was used to verify that each primer pair produced single amplicons, and the identities of the PCR products were verified by cloning and sequencing. qRT-PCR was performed by using either TaqMan fluorescent probes or SYBR green methods.

For the TaqMan method, each 20-μl reaction contained 1 μl of each forward and reverse specific primers (10 μM),1 μl of fluorescent TaqMan probes (5 μM), 10 μl of 2× Universal TaqMan PCR Master Mix, 4 μl of RNase-free water, and 3 μl of template cDNA. The reactions were carried out under the following conditions: 50°C for 2 min and 95°C for 10 min, followed by 40 cycles of 95°C for 15 s and 60°C for 1 min. The target sequences were amplified by using the following primer pairs and probes: Y1 RNA, forward (5′-GGCTGGTCCGAA GGTAGTGA-3′), reverse (5′-AAAAGACTAGTCAAGTGCAGT-3′), and probe (5′-FAM-TGATTGTTCACAGTCAGTTAC-TAMRA-3′); Y3 RNA, forward (5′-GGCTGGTCCGAGTGCAGT-3′), reverse (5′-AAAAGGCTAGTCA AGTGAAGC-3′), and probe (5′-FAM-CACAACCAGTTACAGATT-TAMR A--3′); 7SL RNA,: forward (5′-ATCGGGTGTCCCGCACTAAG-3′), reverse (5′-CACCCCTCCTTAGGCAACCT-3′), and probe 5′-FAM-CATCAATATGGT GACCTCC TAMRA-3′); HIV RNA,: forward (5′-TGTGTGCCCGTCTGTTG TGT-3′), reverse (5′-GAGTCCTGCGTCGAGAGAGC-3′), and probe (5′-FA M-CAGTGGCGCCCGAACAGGGA-TAMRA-3′); and β-actin RNA, forward (5′-TCACCCACACTGTGCCCATCTACGA-3′), reverse (5′-CAGCGGAACC GCTCATTGCCAATGG-3′); and probe (5′-6FAM-ATGCCCTCCCCCATGC CATCCTGCGT-TAMRA-3′). The primer-probe set specific for A3G was a predesigned TaqMan gene expression assay (Applied Biosystems assay identification no. Hs00222415).

For the SYBR green method, each 20-μl reaction mixture contained 1 μl of each forward and reverse specific primers (10 μM), 10 μl of 2× SYBR green PCR Master Mix, 5 μl of RNase-free water, and 3 μl of template cDNA. The reactions were performed under the following conditions: 50°C for 2 min and 95°C for 10 min, followed by 40 cycles of 95°C for 15 s and 60°C for 1 min, followed by a dissociation protocol. Single peaks in the melting-curve analysis indicated specific amplicons. The target sequences amplified by the SYBR green method used the following primer pairs: 5S RNA, forward (5′-TTCAGCGTCT ACGGCCATAC-3′), and reverse (5′-AGCCAAAGAAAAAGCCTAC-3′); Y4 RNA, forward (5′-GGCTGGTCCGATGGTAGTG-3′), and reverse (5′-AAGC CAGTCAAATTTAGCAGTGGG-3′); Y5 RNA, forward (5′-AGTTGGTCCG AGTGTTGTGGGT-3′), and reverse (5′-ACAGCAAGCTAGTCAAGCGCG-3′); tRNA-Phe, forward (5′-GCCGAAATAGCTCAGTTGGGAGA-3′), and reverse (5′-TGGTGCCGAAACCCGG-3′); tRNA-Lys,3 forward (5′-GCCCGG ATAGCTCAGTCG-3′), and reverse (5′-TGGCGCCCGAACAGG-3′); and GAPDH, forward (5′-GCAAATTCCATGGCACCGT-3′), and reverse (5′-TC GCCCCACTTGATTTTGG-3′).

Sensitivity, linearity, range, and quantification by qRT-PCR. The copy numbers of the target cDNA in the qRT-PCR assay were determined by using a standard curve of 10-fold serial dilutions of nonlinearized plasmid DNA containing the target sequence (ranging from 5 or 10 copies to 5×10^5 or 5×10^6 copies). Absolute RNA copy numbers were calculated by using standard dilution curves of plasmids containing the target sequence. If the template cDNA was diluted before being input into the reaction, the copy number of the target transcript was adjusted by the dilution factor. The sensitivity of the assay or limit of detection was determined by the lowest copy number that was consistently amplified within the linear portion of the standard curve. The detection limit ranged from 5 to 50 copies per reaction for the various primer sets. The qRT-PCR assay detected A3G, Y1, Y3, Y4, 7SL, and GAPDH at 5 copies; 5S and tRNA-Lys,3 at 10 copies; and Alu1, tRNA-Phe, and Y5 at 50 copies per reaction. All standards at various concentrations were amplified linearly over a range of at least five orders of magnitude, and the correlation coefficients (r^2) were greater than 0.99. Copy numbers of transcripts were calculated by using standard dilution curves of plasmids containing the target sequence.

RNA end labeling. RNAs coprecipitated with A3G-HA were dissolved in 10 μl of RNase-free water and mixed with 17 μl of a buffer containing 10% dimethyl sulfoxide (Sigma), 1× T4 RNA ligase buffer (Roche), 4 U of recombinant RNasin (Promega), and 10 μg of bovine serum albumin/ml. The RNA molecules were labeled at their 3′ ends by incubation of the reaction mixture with 1 μl of [^{32}P]pCp at 3,000 Ci/mmol (ICN; 1 Ci = 37 GBq, Perkin-Elmer) and 2 μl of T4 RNA ligase at 10 U/μl (Roche) overnight at 10°C. The labeled RNA molecules were then purified with a Sephadex G-50 spin column (Roche), extracted with phenol-chloroform, and precipitated with ethanol after the addition of linear polyacrylamide. The radiolabeled RNA samples were pelleted from the ethanol, dissolved in 10 μl of RNase-free water, and separated on a 10% polyacrylamide–8 M urea gel in Tris-borate-EDTA buffer. The gel was exposed to Kodak BioMax XAR film.

RNA cloning and sequencing. RNA cloning and sequencing were performed according to published protocols, with modifications as described below (1a) In brief, APOBEC3G-binding RNAs or HIV-1 virion-associated RNAs, obtained as described above, were dephosphorylated with calf intestinal alkaline phosphatase at 37°C for 30 min and run on a denaturing polyacrylamide gel alongside an RNA marker. A gel slice around 300 nucleotides long was excised, and the RNA was purified from the gel (QIAGEN). This RNA was then ligated to a phosphorylated 3′ adapter (rUrUrUAACCGCGAATTCCAG-L; A, C, G, and T, DNA residues; rA, rC, rG, and rU, RNA residues; L, 3′ hydroxyl blocking group; Integrated DNA Technologies). The RNA+adapter ligation product was reverse transcribed by using an RT primer-PCR 3′ primer (5′-GACTAGCTGG AATTCGCGGTTAAA-3′) to make the first strand cDNA. Subsequent PCR amplification of the cDNA was performed by using RT primer- PCR 3′ primer and random hexamers (Invitrogen). The PCR product was cloned into a pCR2.1-TOPO vector as described by the manufacturer (Invitrogen) and sequenced.

RNase protection assay. An RNase protection assay was performed as outlined by the manufacturer of the RPA III kit (Ambion). The chimeric riboprobe used was designed to hybridize to part of HIV-1 genomic RNA and also to Y3 RNA. To generate this riboprobe, the cDNA of Y3 RNA was obtained by using the following primer pair: forward, 5′-GGCTGGTCCGAGTGCAGGTGGG-3′, and reverse, 5′-AAAGGCTAGTCAAGTGAAGCAG-3′. The cDNA was cloned into the pCR2.1-TOPO vector to obtain Y3-TOPO. A 200-bp fragment of HIV DNA was amplified from HIV-1pNL4-3 plasmid DNA using the following primers: forward, 5′-GTACAAGCTTATCCCTCAGACCCTTTTAGTCAG-3′ and reverse, 5′-GTACGGATCCCCATCTCTCTCCTTCTAGCCTC-3′ containing HindIII and BamHI sites, respectively. The HIV PCR product was cloned into Y3-TOPO to generate the HIV-Y3-TOPO vector, and the resulting plasmid was confirmed by sequencing. The riboprobe was made by linearizing the HIV-Y3-TOPO vector with HindIII, and T7 RNA polymerase (Invitrogen) was used to generate an antisense transcript of 406 nucleotides. The riboprobe was radiolabeled by including [^{32}P]rCTP (Perkin-Elmer) in the in vitro transcription reaction mixture. The in vitro transcription reaction mixture was purified by phenol-chloroform extractions, followed by chloroform extraction and ethanol precipitation.

RESULTS

Cellular cofactors of A3G. To study the interaction of A3G with cellular proteins, A3G-HA-expressing 293 cells (293/A3G-HA) and parental 293 cells were used (74). Endogenous A3G was not detected in the parental 293 cells (Fig. 1A, lane 2), which are permissive for HIV-1 Vif-defective viruses (Fig. 1B). 293/A3G-HA cells became nonpermissive for HIV-1 Vif-defective viruses (Fig. 1B), and their expression level of A3G-HA (Fig. 1A, lane 3) was comparable to that of endogenous A3G in nonpermissive CD4$^+$ H9 T cells (Fig. 1A, lane 1). Since the A3G-HA in 293/A3G-HA cells was functionally active against HIV-1, we examined the interaction of cellular proteins with A3G-HA by coimmunoprecipitation analysis. An anti-HA antibody conjugated to agarose beads immunoprecipitated HA-tagged A3G from lysates of 293/A3G-HA cells (Fig. 1C, lane 1) but not control 293 cells (Fig. 1C, lane 2). In repeat experiments, two cellular proteins coprecipitated with A3G-HA (Fig. 1C, lane 1). These proteins, of ~60 and ~48 kDa (Fig. 1C), were identified by mass spectrometry as Ro60
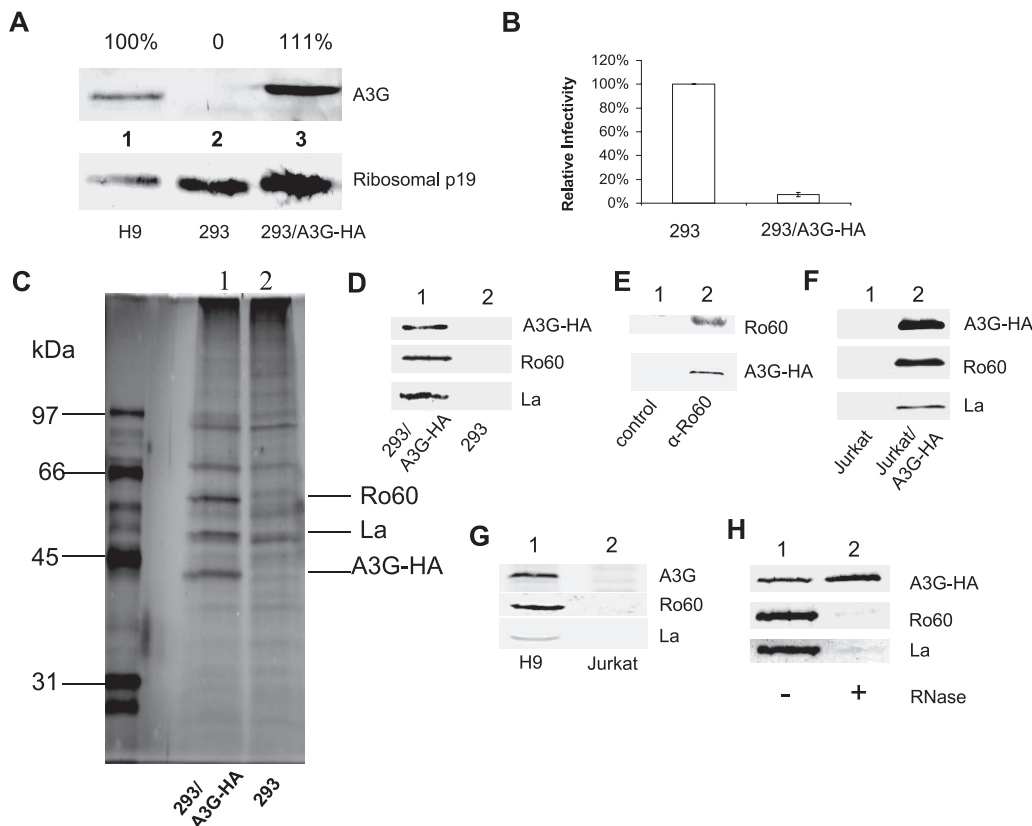
FIG. 1. Characterization of 293/A3G-HA cells and interaction of cellular factors with A3G. (A) The level of A3G-HA in 293/A3G-HA cells was similar to that of endogenous A3G in H9 cells. Endogenous A3G was not detected in 293 cells. (B) A3G-HA in 293/A3G-HA cells had potent anti-HIV-1 activity. (C) Coimmunoprecipitation of cellular proteins with A3G-HA. Cell lysates from 293/A3G-HA or 293 cells were immunoprecipitated with anti-HA antibody conjugated to agarose beads, followed by SDS-PAGE and silver staining. The identification of Ro60 and La antigen coprecipitated with A3G-HA was achieved by mass spectroscopic analysis; these proteins were not detected in the control 293 samples. (D) Immunoblot of precipitated samples from 293/A3G-HA or 293 cells. Precipitated samples prepared as described above were separated by SDS-PAGE, transferred to nitrocellulose membranes, and reacted with antibodies to Ro60, La, or HA for the detection of A3G-HA. (E) Co-immunoprecipitation of A3G-HA with endogenous Ro60. Cell lysates from 293/A3G-HA cells were immunoprecipitated with a mouse anti-Ro60 antibody or a control mouse anti-myc antibody. Precipitated samples were separated by SDS-PAGE, transferred to nitrocellulose membranes, and reacted with antibodies to Ro60 or HA for the detection of A3G-HA. (F) Coimmunoprecipitation of Ro60 and La with A3G-HA expressed in CD4$^+$ Jurkat cells. Cell lysates from Jurkat/A3G-HA or Jurkat cells were immunoprecipitated with anti-HA antibody conjugated to agarose beads. Precipitated samples were separated by SDS-PAGE, transferred to nitrocellulose membranes, and reacted with antibodies to Ro60, La, or HA for the detection of A3G-HA. (G) Coimmunoprecipitation of Ro60 and La with endogenous A3G expressed in CD4$^+$ H9 cells. Cell lysates from H9 or Jurkat cells were immunoprecipitated with the anti-A3G antibody. Precipitated samples were separated by SDS-PAGE, transferred to nitrocellulose membranes, and reacted with antibodies to Ro60, La, or A3G. (H) Coimmunoprecipitation of Ro60 and La with A3G was RNase sensitive.

and the La antigen, respectively. Their identities were confirmed by reactivity with Ro60- or La-specific antibodies (Fig. 1D, lane 1). Reciprocal immunoprecipitation of Ro60 also coprecipitated A3G-HA (Fig. 1E, lane 2). Interaction of A3G with Ro60 and La has recently been reported by other groups (12, 20, 30). In addition to Ro60 and La, PABP1 was also found to interact with A3G (data not shown), a finding consistent with a recent report (30).

Expression of A3G-HA in Jurkat/A3G-HA CD4$^+$ T cells also resulted in an association with Ro60 or La (Fig. 1F, lane 2). Interaction of endogenous A3G in H9 CD4$^+$ T cells with Ro60 or La by immunoprecipitation with an antibody against A3G (Fig. 1G, lane 1) was also observed. Interaction of A3G with Ro60 or La (Fig. 1H, lane 1) was largely abolished by RNase treatment (Fig. 1H, lane 2), suggesting that cellular RNAs mediate the interaction between A3G and Ro60 or La.

To examine the association of cellular RNAs with A3G, A3G-HA-coprecipitated samples from 293/A3G-HA cell lysates were analyzed by qRT-PCR using primers specific for Y RNAs, tRNA-Phe, tRNA-Lys,3, 5S rRNA, Alu RNAs, GAPDH mRNA, A3G mRNA, and 7SL RNA. Copy numbers of these coprecipitated RNAs were then determined. Cell lysates from 293 cell lysates were also examined side by side as the negative control to determine the nonspecific binding of various RNAs from the 293 samples to the assay system. Among the Y RNAs, A3G interacted efficiently with Y1, Y3, and Y4 RNAs compared to the control 293 samples (Fig. 2A). However, the interaction of A3G with Y5 RNA was inefficient (Fig. 2A), even though the amounts of Y4 and Y5 RNAs were comparable in 293/A3G-HA cell lysates (data not shown). An efficient interaction was also detected between A3G and 7SL RNA by qRT-PCR (Fig. 2A). The interaction between A3G
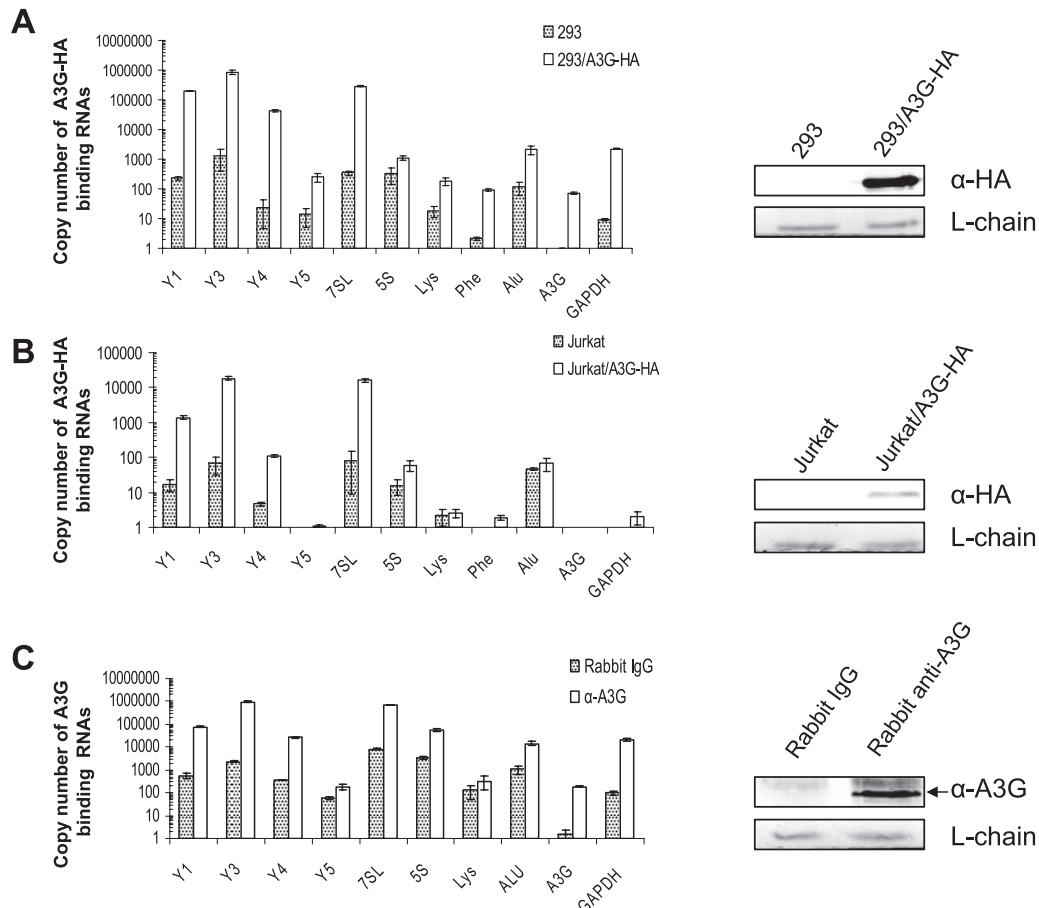
FIG. 2. Selective interaction of A3G with 7SL and Y RNAs. (A) Analysis of the interactions of cellular RNAs with A3G-HA by qRT-PCR. Cell lysates from 293/A3G-HA or 293 cells were immunoprecipitated with anti-HA antibody conjugated to agarose beads. RNAs were extracted from coprecipitated samples and analyzed by qRT-PCR using primers specific for Y1, Y3, Y4, Y5, 7SL RNA, 5S rRNA, Alu RNAs, A3G mRNA, GAPDH mRNA, tRNA-Phe, or tRNA-Lys,3. Copy numbers of various RNAs coprecipitated with A3G-HA from 8.52×10^3 293/A3G-HA cells are shown. Nonspecific binding of RNAs to the immunoprecipitation system by the negative control 293 samples was also determined. (B) Interaction of cellular RNAs with A3G-HA in Jurkat/A3G-HA cells. Cell lysates from Jurkat/A3G-HA or Jurkat (A3G-negative) cells were immunoprecipitated with anti-HA antibody conjugated to agarose beads. RNAs were extracted from coprecipitated samples and analyzed by qRT-PCR using primers specific for Y1, Y3, Y4, Y5, 7SL RNA, 5S rRNA, Alu RNAs, A3G mRNA, GAPDH mRNA, tRNA-Phe, or tRNA-Lys,3. Copy numbers of various RNAs coprecipitated with A3G-HA from 1.71×10^3 Jurkat/A3G-HA cells are shown. Nonspecific binding of RNAs to the immunoprecipitation system by the negative control Jurkat samples was also determined. (C) RNA immunoprecipitation with endogenous A3G from CD4^{+} T cells. Portions (10 μg) of bivalent anti-CD3/8 antibody (Johnson Wong) were added to 2.0×10^7 freshly isolated PBMC in 10 ml of R-10 medium with 10 IU of IL-2 (Roche)/ml. The bivalent antibody depletes CD8 cells and stimulates the outgrowth of CD4 cells from the culture. After 2 days, 10 ml of additional R-10 medium containing IL-2 (10 IU/ml) was added. After 5 days total in culture, coimmunoprecipitation with anti-A3G or rabbit immunoglobulin G (IgG) (mock) was performed, and RNA was isolated from coprecipitated samples. Various RNAs coprecipitated with A3G or mock IgG were detected by qRT-PCR. Copy numbers of the various RNAs coprecipitated with A3G-HA from 4.5×10^3 cells are shown. Nonspecific binding of RNAs to the immunoprecipitation system by the negative control (mock) samples was also determined.

and selected polymerase III (Pol III)-derived RNAs was not random, since the abundant 5S rRNA did not interact efficiently with A3G-HA (Fig. 2A). The interaction of A3G with Pol III-transcribed Alu RNA, tRNA-Phe, or tRNA-Lys,3 was also much weaker (>100-fold less) than that with the Y1, Y3, or 7SL RNAs (Fig. 2A). Interaction of A3G with cellular mRNAs, including A3G mRNA, has been reported (12, 20, 30, 67). However, the copy number of 7SL RNA coprecipitated with A3G-HA was >400-fold higher than that of A3G mRNA and >100-fold higher than that of GAPDH mRNA (Fig. 2A).

The interaction of A3G-HA in CD4^{+} T cells (Jurkat/A3G-HA) with Pol III-derived RNAs was also examined; Jurkat

cells that did not express A3G were used as negative controls. An efficient interaction between A3G-HA and Y1, Y3, and 7SL RNAs was detected (Fig. 2B). Interaction between A3G-HA and 5S rRNA, tRNAs, Alu RNAs, Y5 RNA, A3G mRNA, or GAPDH mRNA was again less efficient (>100-fold less) than that with 7SL RNA in Jurkat/A3G-HA cells (Fig. 2B). Efficient interactions between endogenous A3G and 7SL or Y3 RNAs were also detected in primary CD4^{+} T cells (Fig. 2C).

RNAs coprecipitated with A3G-HA were also analyzed by end labeling (Fig. 3A). A prominent band of approximately 300 nucleotides was detected in A3G-HA-coprecipitated sam-
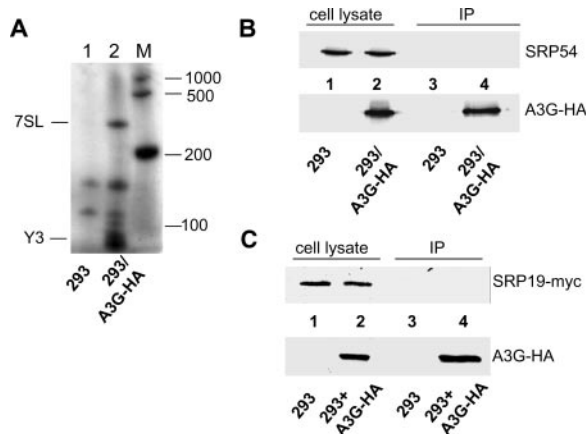
FIG. 3. Further characterization of cellular factors that interact with A3G-HA. (A) Analysis of A3G-HA-coprecipitated RNA content by RNA end labeling. Cell lysates from 293/A3G-HA and 293 cells were immunoprecipitated with anti-HA antibody conjugated to agarose beads. RNAs were extracted from coprecipitated samples and end labeled with T4 RNA ligase and [^{32}P]pCp. RNA samples were analyzed on a denaturing polyacrylamide–8 M urea gel in Tris-borate-EDTA buffer. (B) Endogenous SRP54 was not coprecipitated with A3G-HA from 293/A3G-HA cells. (C) SRP19-myc was not coprecipitated with A3G-HA from transfected 293 cells.

ples from 293/A3G-HA cells (Fig. 3A, lane 2) but not in the control 293 cell samples (Fig. 3A, lane 1). Sequencing analysis identified this RNA species as 7SL RNA. The RNA bands just below 100 nucleotides were also sequenced, and Y3 RNA was the predominant RNA (24 of 25 clones) identified. The RNA end labeling and RNA sequencing analysis were consistent with the qRT-PCR results and indicated that 7SL and Y3 RNAs were the most abundant RNAs that interacted with A3G. Although A3G interacted with both Y RNAs and the Y RNA-binding Ro60 proteins (Fig. 1), it did not interact with endogenous SRP54 protein, which associates with 7SL RNA and other SRP proteins to form SRP complexes, in 293 cells (Fig. 3B). Interaction of A3G-HA with SRP19-myc in transfected 293 cells was also not detected (Fig. 3C). These data indicated that A3G interacted with 7SL RNAs that were not part of the SRP RNP complexes.

Among A3G-interacting Pol III RNAs, 7SL RNA, but not Y RNA, is preferentially packaged into HIV-1 virions. A3G packaging into HIV-1 virions requires the NC domain of the HIV-1 Gag protein and unidentified RNA(s). The fact that A3G selectively interacted with 7SL and certain Y RNAs raised the question of whether these RNAs could mediate virion packaging of A3G. To address this question, HIV-1 virions in the culture supernatants of NL4-3-transfected 293T cells were purified and analyzed for Y and 7SL RNAs by qRT-PCR. As a control for nonspecific secretion of cellular RNAs into the culture supernatants, supernatants from mock-transfected 293T cells were also prepared in the same fashion and analyzed. The copy number of the 7SL RNA in HIV-1 virions was ~13-fold higher than that of HIV-1 RNA (Fig. 4A). However, the copy numbers of Y1, Y3, or Y4 RNAs in HIV-1 virions were >50-fold less than that of HIV-1 RNA (Fig. 4A). Thus, assuming two copies of viral RNA per HIV-1 particle, Y RNAs

are likely to be packaged at far below one copy per HIV-1 particle.

To further compare the relative abundances of Y RNAs and HIV-1 RNA in HIV-1 virions, RNAs from purified HIV-1 virions were also analyzed by RNase protection assay using an RNA probe with complementarities to both HIV-1 and Y3 RNA sequences. In HIV-1-transfected cells, a 200-nucleotide riboprobe fragment corresponding to sequences from HIV-1 RNA and a 101-nucleotide riboprobe fragment corresponding to sequences from Y3 RNA were detected (Fig. 4B, lane 1). As expected, only the Y3 RNA fragment, and not the HIV-1 RNA fragment, was detected in the mock-transfected cells (Fig. 4B, lane 2). RNAs purified from HIV-1 virions generated only the HIV-1 RNA fragment (Fig. 4B, lane 3), indicating that Y3 RNA was packaged at a much lower level than was HIV-1 RNA. As expected, no fragment was detected in the control samples generated from the supernatant of mock-transfected cells (Fig. 4B, lane 4). Similar results were also observed for Y1 RNA (data not shown). The RNA protection data were consistent with the qRT-PCR results (Fig. 4A), indicating that Y RNAs are not efficiently packaged into HIV-1 virions.

The inefficient packaging of Y RNAs, compared to 7SL RNA, could not be attributed to the lower intracellular abundance of Y RNAs. We also compared the relative efficiency of virion packaging of the A3G-interacting RNAs. It is known that cellular mRNAs such as β-actin mRNA are not selectively packaged into HIV-1 virions (53). When the efficiency of β-actin mRNA packaging (copies of β-actin mRNA in HIV-1 virions/copies of β-actin mRNA in virus-producing cells) was set to 1, the packaging of 7SL RNA was found to be several thousandfold more efficient than that of β-actin mRNA (Fig. 4C), a finding consistent with the previous report that 7SL RNA is more selectively packaged into HIV-1 virions than is β-actin mRNA (53). Packaging of 7SL RNA was also more selective (>100-fold more efficient) than that of Y1 or Y3 RNA (Fig. 4C). Collectively, these data indicate that A3G interacts selectively with 7SL and certain Y RNAs in virus-producing cells but that Y RNAs are packaged poorly in HIV-1 virions.

To further examine the packaging of 7SL RNAs into HIV-1 virions, RNAs in purified HIV-1 virions were also analyzed by end labeling and compared to the end-labeled RNAs of A3G-HA-coprecipitated samples from 293/A3G-HA cells (Fig. 4D). Among the A3G-interacting RNAs (Fig. 4D, lane 5), the 300-nucleotide RNA was the predominant RNA detected in HIV-1 virions (Fig. 4D, lane 3). This RNA species was cloned and sequenced and identified as 7SL RNA. Compared to 7SL RNA, packaging of other A3G-binding RNAs such as Y3 RNA into HIV-1 virions was less efficient (Fig. 4D, lane 3). In addition to 7SL RNA, HIV-1 virions also contained abundant tRNAs and an unidentified RNA species between 100 and 200 nucleotides (Fig. 4D, lane 3, arrow). The pattern of low-molecular-weight RNAs detected in our HIV-1 virion samples was very similar to that observed in a previous study (26).

The NC domain of HIV-1 Gag is required for 7SL RNA packaging. Packaging of A3G into virus requires the RNA-binding NC domain of HIV-1 Gag and unidentified RNAs (1, 9, 15, 28, 39, 51, 56, 64, 76). Since A3G interacts with 7SL RNA, which is selectively packaged into HIV-1 virions, it is intriguing to speculate that 7SL RNA mediates A3G virion
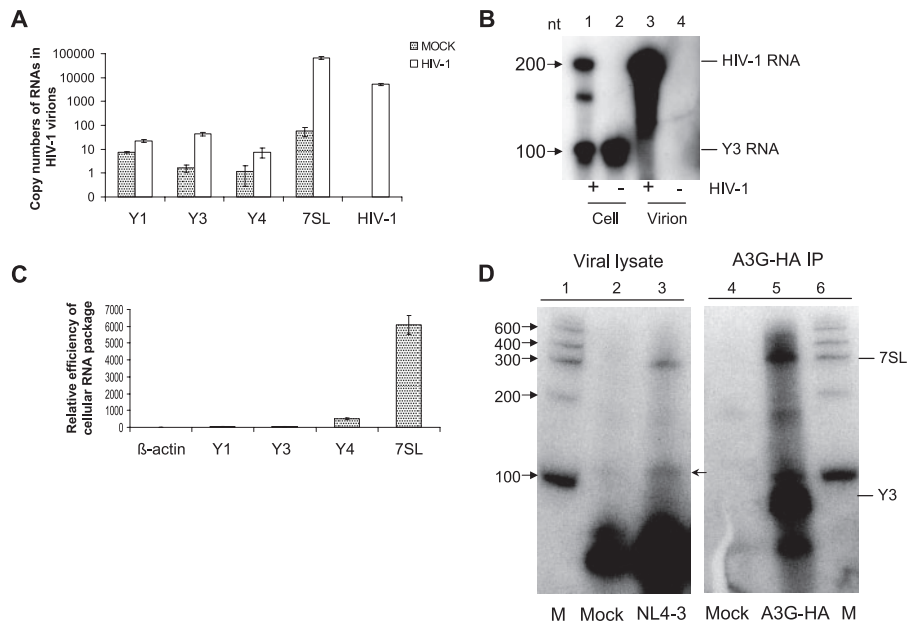
FIG. 4. Analysis of the packaging of Y and 7SL RNAs into HIV-1 virions. (A) Detection of Y and 7SL RNAs in purified HIV-1 virions. HIV-1 virions in the culture supernatants of NL4-3-transfected 293T cells were purified by sucrose density gradient centrifugation. Virion-associated RNAs were analyzed by qRT-PCR using specific primers for Y1, Y3, Y4, or 7SL RNA. Similar samples from mock-transfected 293T cells were prepared and analyzed side by side to determine non-virus-mediated secretion of Y and 7SL RNAs. The copy numbers of RNAs detected in HIV-1 virions from 5 pg of p24 equivalent culture supernatant are shown. (B) RNA samples from mock- or NL4-3-transfected 293T cells or purified virions were analyzed by a RNase protection assay. Cell-associated or virion-associated RNAs were extracted by using TRIzol (Invitrogen). In HIV-1-transfected cells (lane 1), a 200-nucleotide riboprobe fragment corresponding to sequences from HIV-1 RNA and a 101-nucleotide riboprobe fragment corresponding to sequences from Y3 RNA were detected. Only the Y3 RNA fragment, and not the HIV-1 RNA fragment, was detected in the mock-transfected cells (lane 2). RNAs purified from HIV-1 virions generated only the HIV-1 RNA fragment and not the Y3 RNA fragment (lane 3). (C) Relative efficiency of virion packaging of RNAs analyzed by qRT-PCR. The efficiency of RNA packaging was evaluated by comparing the ratio of the number of copies of a particular RNA in HIV-1 virions to the number of copies of the same RNA in virus-producing cells. The efficiency of β-actin mRNA packaging was set to 1. (D) RNAs from purified HIV-1 virions or mock control samples were analyzed by end labeling. The end-labeled RNAs of A3G-HA coprecipitated samples from A3G-HA-transfected 293T cells (lane 5) were used for comparison.

packaging. If this were the case, one might expect that 7SL RNA packaging should also be NC dependent. To examine whether 7SL RNA could be packaged into HIV-1 particles through an NC-dependent mechanism, we used the HIV-1 constructs BH10.FS−.Vif− (NC positive) and Zwt-p6.Vif− (NC replaced by a yeast leucine zipper domain) (9). Comparable amounts of viral particles with or without NC were produced from transfected 293T cells (Fig. 5A). Viral particle-associated RNAs were extracted and analyzed by qRT-PCR using 7SL RNA-specific primers. While 7SL RNAs were specifically packaged into BH10.FS−.Vif− particles, compared to the mock-transfected 293T cell control (the nonspecific secretion of 7SL RNA in the mock controls was <5% of that in the BH10.FS−.Vif− particles), the 7SL RNAs were poorly packaged (a > 80% reduction) into Zwt-p6.Vif− particles (Fig. 5B). The influence of the NC domain on 7SL RNA packaging was not affected by the presence of Vif (Data not show). On the other hand, tRNA-Lys,3 or tRNA-Phe packaging was not significantly influenced by NC (Fig. 5B). A3G virion packaging into Zwt-p6.Vif− particles was reduced by ca. 90% compared to the BH10.FS−.Vif− particles (9). These data suggest that 7SL RNA, but not tRNAs, can mediate A3G virion packaging.

Inhibition of 7SL RNA packaging reduces A3G virion packaging and its antiviral function. 7SL RNA is part of the signal
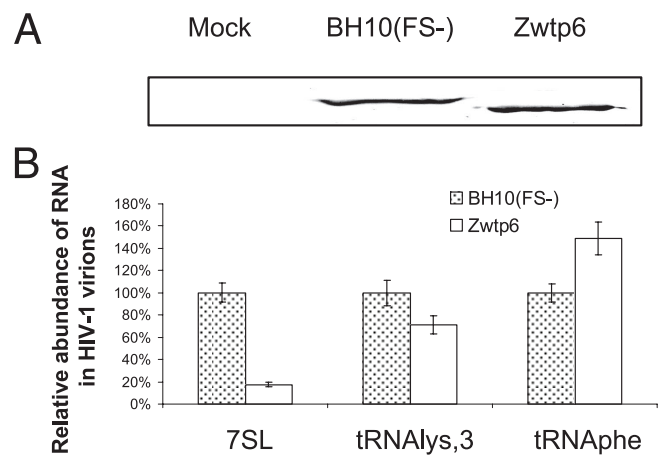

FIG. 5. The NC domain of HIV-1 Gag is required for 7SL RNA packaging. (A) NC+ (BH10FS-Vif−) and NC− (Zwtp6Vif−) HIV-1 particles were produced from transfected 293T cells and analyzed by immunoblotting with the anti-p24 antibody. (B) Influence of NC deletion on 7SL RNA packaging. RNAs associated with NC+ (BH10FS−) and NC− (Zwtp6) HIV-1 particles were extracted and analyzed by qRT-PCR. The efficiency of RNA packaging into BH10FS−Vif− was set to 100%.
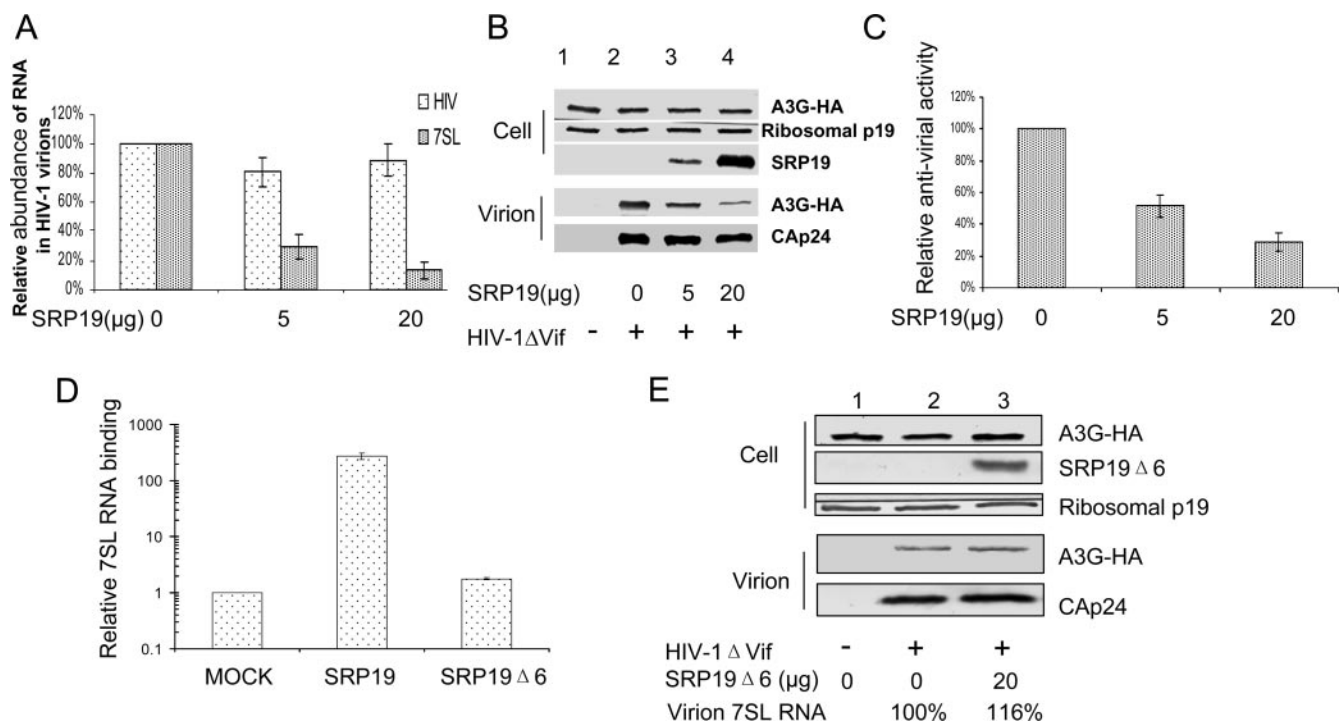
FIG. 6. Overexpression of SRP19 proteins impairs 7SL RNA, as well as A3G, encapsidation. (A) Overexpression of SRP19-myc protein impaired 7SL RNA but not viral genomic RNA packaging into HIV-1 virions. HIV-1 virions were produced from transfected 293T cells in the absence or presence of increasing amounts of exogenous SRP19-myc proteins. Virion-associated RNAs were analyzed by qRT-PCR. The level of viral genomic RNA or 7SL RNA in HIV-1 virions in the absence of exogenous SRP19 was set to 100%. (B) Overexpression of SRP19 proteins inhibited A3G encapsidation into HIV-1 virions. HIV-1ΔVif virions plus A3G-HA were produced from transfected 293T cells in the absence or presence of increasing amounts of exogenous SRP19-myc proteins. Packaging of A3G-HA into HIV-1ΔVif virions was analyzed by immunoblotting. A3G-HA was detected with the anti-HA antibody, viral Gag proteins were detected with an anti-p24 antibody, and SRP19-myc proteins were detected with an anti-myc MAb. Secretion of A3G-HA in the absence of HIV-1ΔVif was used as a negative control (lane 1). (C) Overexpression of SRP19 proteins reduced the antiviral activity of A3G against HIV-1. The antiviral activity of A3G-HA in the absence of exogenous SRP19 was set to 100%. (D) SRP19Δ6 showed a reduced ability to interact with 7SL RNA. Cell lysates from SRP19-myc or SRP19Δ6myc expression vector-transfected 293T cells were immunoprecipitated with the anti-myc antibody. RNAs were extracted from coprecipitated samples, reverse transcribed, and analyzed by qRT-PCR using 7SL RNA-specific primers. Cell lysates from mock-transfected 293T cells were used as a negative control for the nonspecific binding of 7SL RNA to the assay system and set to 1. (E) Overexpression of SRP19Δ6 proteins did not inhibit A3G-HA encapsidation into HIV-1 virions. HIV-1ΔVif virions plus A3G-HA were produced from transfected 293T cells in the absence or the presence of exogenous SRP19Δ6 proteins. Packaging of A3G-HA into HIV-1ΔVif virions was analyzed by immunoblotting. A3G-HA and viral Gag proteins were detected as described above. Viral Gag proteins were detected with an anti-p24 antibody, and SRP19Δ6-myc proteins were detected with an anti-myc MAb. Secretion of A3G-HA in the absence of HIV-1ΔVif was used as a negative control (lane 1). Overexpression of SRP19Δ6 proteins did not impair 7SL RNA packaging into HIV-1 virions. The level of 7SL RNA in HIV-1ΔVif virions in the absence of exogenous SRP19Δ6 was set to 100%.

recognition particle (SRP) RNP complex, which also contains one copy each of the SRP72, SRP68, SRP54, SRP19, SRP14, and SRP9 proteins. 7SL RNA, but not the SRP proteins, is packaged into HIV-1 virions (53), suggesting that HIV-1 packages free 7SL RNA but not with the 7SL RNA that is part of an SRP RNP complex. A3G interacted with 7SL RNA but not the SRP54 or SRP19 proteins (Fig. 3). It is likely that A3G interacts with free 7SL RNA but not with 7SL RNA that is part of an SRP RNP complex. Thus, promoting the formation of SRP complexes may limit the 7SL RNA interaction with A3G and reduce 7SL RNA packaging into HIV-1 virions. SRP19 plays a critical role in promoting the formation of SRP RNP complexes containing 7SL RNA (18). We reasoned that overexpression of SRP19 proteins might promote the participation of 7SL RNA in the formation of SRP complexes and reduce its packaging into HIV-1 virions. In addition to promoting 7SL RNA participation in SRP RNP formation, SRP19 could bind

non-SRP-associated 7SL RNA and interfere with its recognition by HIV-1 Gag, thus reducing 7SL RNA virion packaging (i.e., through a competitive mechanism). Alternatively, it has recently been reported that binding of SRP19 proteins to 7SL RNAs can induce conformational changes in 7SL RNA (48). The changes in 7SL RNA conformation induced by SRP19 might also inhibit its interaction with the HIV-1 Gag or A3G proteins.

Overexpression of SRP19 indeed reduced the packaging of 7SL RNA into HIV-1 virions in a dose-dependent fashion (Fig. 6A). At a 4:1 ratio of plasmid transfection (SRP19 to HIV-1), 7SL RNA packaging was reduced by ca. 90% (Fig. 6A); in contrast, packaging of HIV-1 genomic RNA was not significantly affected by SRP19 overexpression (Fig. 6A). At the same time, A3G packaging was reduced by ~80% at a 4:1 ratio of SRP19 to HIV-1 (Fig. 6B). Consequently, overexpression of SRP19 also reduced the antiviral activity of A3G against
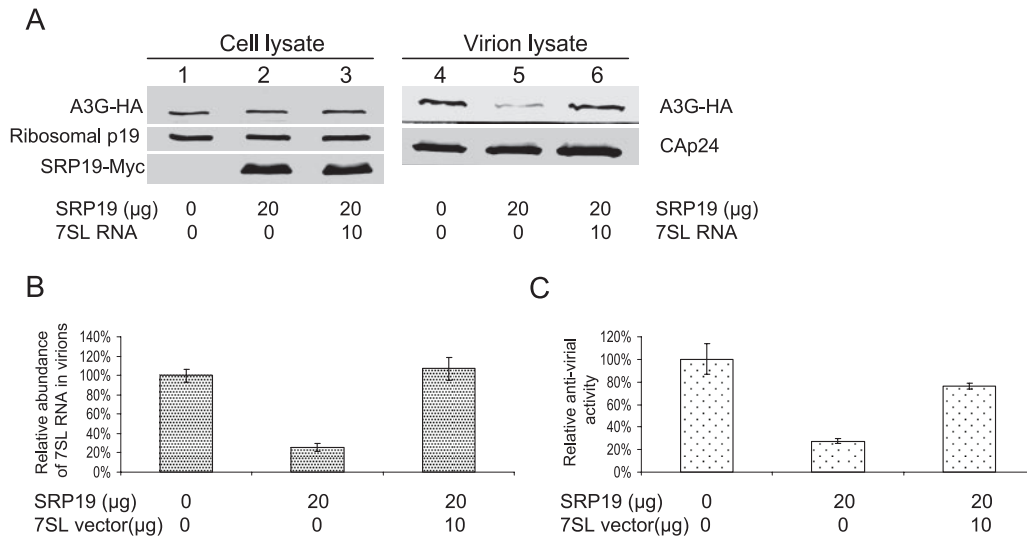
FIG. 7. Impairment in 7SL RNA and A3G encapsidation by SRP19 overexpression is reversed by exogenous 7SL RNA expression. (A) Over-expression of SRP19 proteins inhibited A3G encapsidation into HIV-1 virions and was overcome by exogenous 7SL RNA expression. HIV-1ΔVif virions plus A3G-HA were produced from transfected 293T cells in the absence or presence of exogenous SRP19-myc proteins plus exogenous 7SL RNA (lanes 3 and 6). Packaging of A3G-HA into HIV-1ΔVif virions was analyzed by immunoblotting. A3G-HA was detected with the anti-HA antibody, viral Gag proteins were detected with an anti-p24 antibody, and SRP19-myc proteins were detected with an anti-myc antibody. (B) Virion-associated 7SL RNA. (C) SRP19 protein reduced the antiviral activity of A3G against HIV-1, and this effect was suppressed by exogenous 7SL RNA expression. The antiviral activity of A3G-HA in the absence of exogenous SRP19 was set to 100%.

HIV-1 (Fig. 6C). At a 4:1 ratio (SRP19 [20 μg] to HIV-1[5 μg]), A3G antiviral function was reduced by ~75% (Fig. 6C). In the absence of A3G, HIV-1 infectivity (with or without Vif) was not significantly altered by overexpression of SRP19 (data not shown). Attempts to achieve a more potent effect of the SRP19 overexpression by using a larger quantity of SRP19 expression plasmid posed technical challenges, since both

HIV-1 protein and A3G-HA protein expression were reduced (data not shown). Overexpression of SRP54 also inhibited the interaction between 7SL RNA and A3G, reduced the virion packaging of A3G, and impaired the antiviral activity of A3G (data not shown).

Consistent with the fact that amino acids 8 to 13 of SRP19 have been shown to bind 7SL RNA (54), we found that an
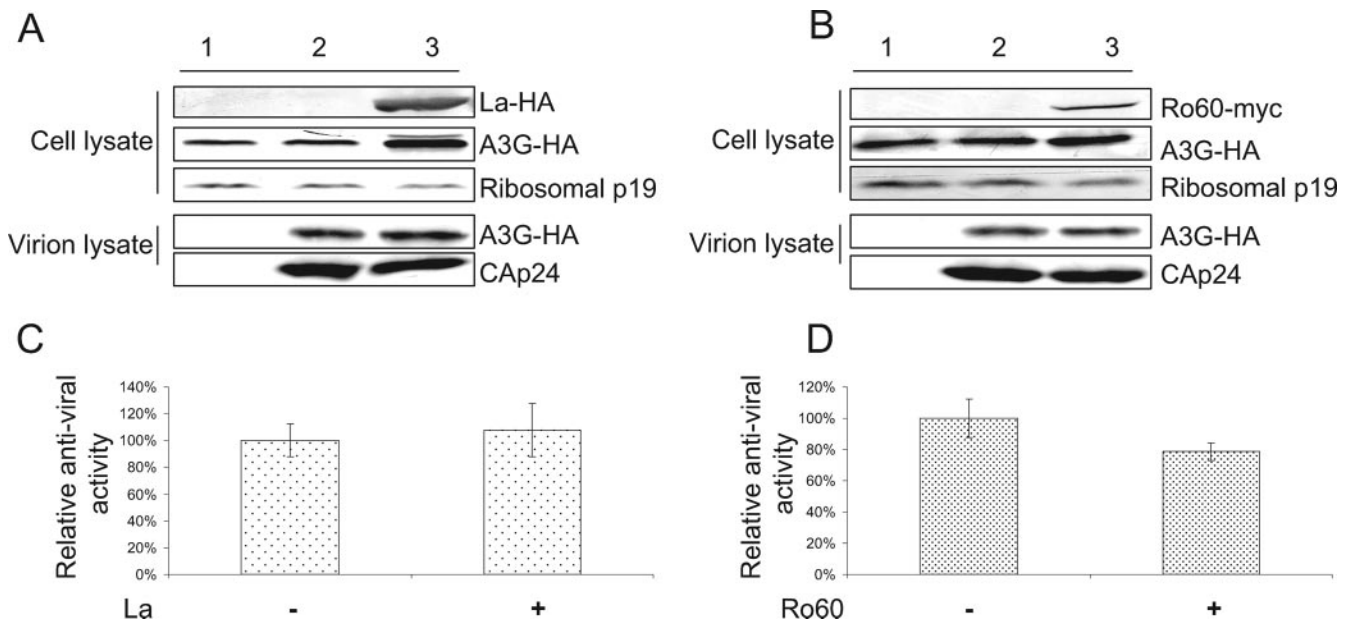

FIG. 8. Overexpression of La-HA (A) or Ro60-myc (B) proteins did not affect A3G-HA virion packaging. HIV-1ΔVif (5 μg of DNA) plus A3G-HA (1 μg) were transfected into 293T cells (T-75 flask) in the absence or presence of La-HA or Ro60-myc expression vector (20 μg). HIV-1ΔVif virions were analyzed by immunoblotting to examine A3G-HA virion packaging. (C and D) HIV-1ΔVif virions were also analyzed by MAGI assay. The antiviral activity of A3G-HA in the absence of exogenous La or Ro60 was set to 100%.
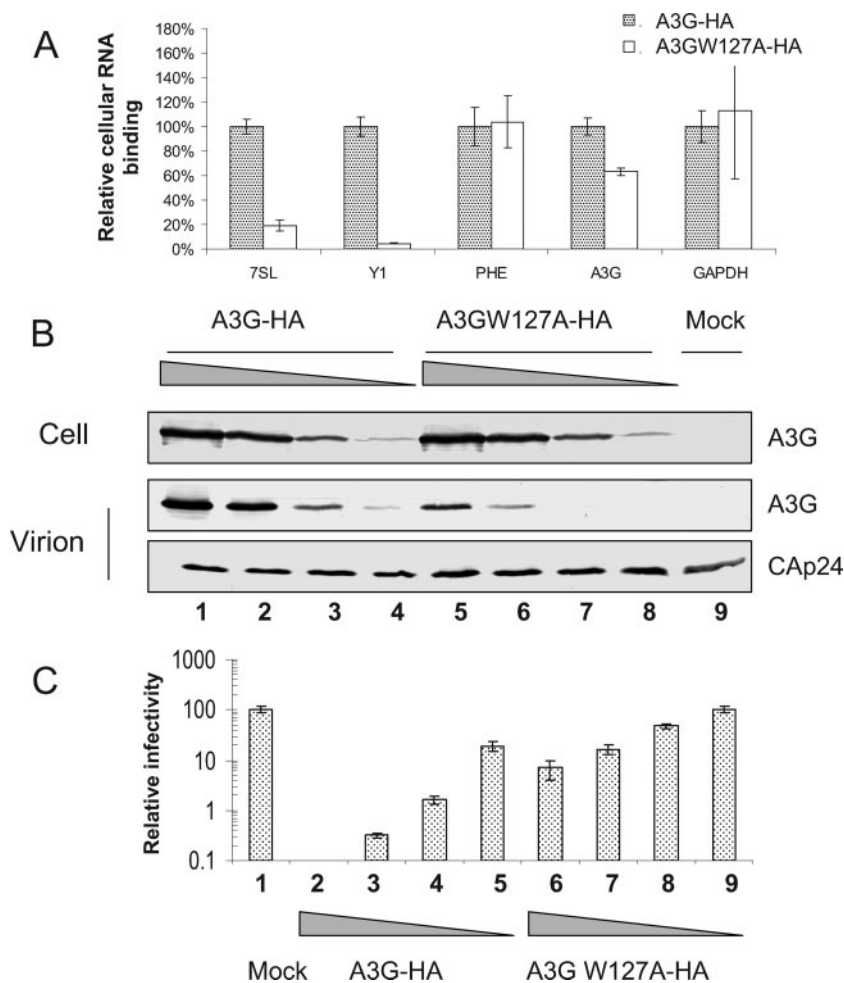
FIG. 9. A3GW127A defective for binding to 7SL RNA are excluded from HIV-1 virions. (A) Interaction of A3G-HA and the A3GW127A-HA mutant with RNAs. 293T cells were transfected with A3G-HA or A3GW127A-HA mutant expression vector. Cell lysates from transfected cells were immunoprecipitated with anti-HA antibody conjugated to agarose beads. RNAs were extracted from coprecipitated samples and analyzed by qRT-PCR using primers specific for Y1, 7SL RNA, tRNA-Phe, A3G mRNA, or GAPDH mRNA. RNA interaction with parental A3G was set to 100%. (B) A3GW127A was defective for virion packaging. HIV-1ΔVif virions (4 μg) were generated from transfected 293T cells in T25 flasks plus decreasing amounts of A3G-HA (4 μg [lane 1], 1 μg [lane 2], 0.25 μg [lane 3], or 0.625 μg [lane 4]) or decreasing amounts of A3GW127A-HA (4 μg [lane 5], 1 μg [lane 6], 0.25 μg [lane 7], or 0.625 μg [lane 8]). Cell lysates and viruses were purified and analyzed by immunoblotting at 48 h after transfection. Parental A3G-HA and mutant A3GW127A-HA proteins were detected with the anti-HA antibody, and viral Gag proteins were detected with an anti-p24 antibody. (C) A3GW127A-HA showed reduced antiviral activity against HIV-1 compared to the parental A3G-HA. HIV-1ΔVif was cotransfected with various amounts of A3GW127A-HA or A3G-HA expression vector as described above. At 48 h posttransfection, virus supernatants were collected and tested in the MAGI assay. Virus infectivity in the absence of A3G-HA or A3GW127A-HA was set to 100%.

in-frame deletion of these 6 amino acids in SRP19 (SRP19Δ6) impaired its interaction with 7SL RNA by >50-fold compared to the native SRP19 (Fig. 6D). Unlike SRP19, at a 4:1 ratio (SRP19Δ6 [20 μg] to HIV-1 [5 μg]), SRP19Δ6 did not inhibit 7SL RNA packaging into HIV-1 virions (Fig. 6E). Also, A3G virion packaging was not affected by overexpression of SRP19Δ6 (Fig. 6E).

Inhibition of A3G virion packaging by overexpression of SRP19 proteins could be reversed by providing additional 7SL RNA to virus-producing cells (Fig. 7), suggesting that the inhibitory effect of SRP19 overexpression on A3G virion packaging is due to a limitation in the amount of 7SL RNA in virus-producing cells. Overexpression of other A3G-associated proteins, such as La-HA (Fig. 8A) or Ro60-myc (Fig.

8B), did not affect A3G-HA virion packaging or the antiviral activity of A3G-HA against HIV-1ΔVif viruses (Fig. 8C and D).

Packaging-defective A3G mutant proteins show impaired 7SL RNA association. To extend our analysis of the role of 7SL RNA in mediating A3G virion packaging, we examined the interaction of packaging-defective A3GW127A mutant (24, 78) with 7SL RNA. A3GW127A showed an ~80% reduction in 7SL RNA binding compared to the parental A3G (Fig. 9A). Its interaction with several other RNAs tested, including GAPDH mRNA, A3G mRNA, or tRNA-Phe, was not significantly compromised compared to that of A3G.

When we compared the virion packaging of the two forms of A3G, we saw more efficient packaging of A3G (Fig. 9B, lanes

1 to 4) than of A3GW127A (Fig. 9B, lanes 5 to 8) into HIV-1 virions. The virion packaging of A3GW127A was about four- to sixfold less efficient than that of A3G (Fig. 9B). The antiviral activity of A3GW127A was significantly weaker than that of the parental A3G (Fig. 9C), a finding consistent with its reduced level of virion packaging.

DISCUSSION

The data presented in this study indicate that certain Pol III-transcribed RNAs, such as 7SL and Y3 RNAs, are preferentially recognized by the cytidine deaminase A3G. Among these A3G-interacting Pol III RNAs, 7SL RNA is the most abundant RNA packaged into HIV-1 virions, even in the absence of A3G. Virion packaging of 7SL RNA is mediated by the Gag molecule and is independent of viral genomic RNA (1, 9, 15, 39, 51, 56, 76). However, the encapsidation of 7SL RNA, as well as A3G, into HIV-1 virions requires the NC domain of HIV-1 Gag (Fig. 5). Thus, the association of A3G with 7SL RNA provides an efficient means of targeting this potent antiviral protein into HIV-1 virions. Consistent with this idea, inhibition of 7SL RNA packaging reduced A3G virion packaging and its antiviral function (Fig. 6). Also, the A3GW127A mutant, which had selectively lost the ability to interact with 7SL RNA but maintained the ability to interact with mRNA and tRNAs (Fig. 8), was defective in virion packaging and had impaired anti-HIV-1 activity.

The majority of intracellular 7SL RNAs are present in the form of SRP RNP complexes (18), which consist of one copy of 7SL RNA and one copy of each of the six SRP proteins (SRP72, SRP68, SRP54, SRP19, SRP14, and SRP9). Free, but not SRP complex-associated 7SL RNA, is packaged into HIV-1 virions (53). SRP19 has been shown to promote the formation of SRP RNP complexes (18). SRP19 binds the S domain of 7SL RNA (18) and could induce conformational changes in 7SL RNA (48). Thus, it is also possible that the binding of SRP19 to 7SL RNA interferes with HIV-1 Gag and/or A3G recognition of 7SL RNA. Overexpression of SRP19 proteins reduced the packaging of 7SL RNA into HIV-1 virions (Fig. 6). Overexpression of SRP19 proteins, as well as SRP54 or SRP9/14, also reduced the interaction between A3G and 7SL RNA. Consequently, overexpression of SRP19 or other SRP proteins decreased the packaging of A3G into HIV-1 virions. More importantly, overexpression of SRP19 reduced A3G antiviral activity. When extra 7SL RNA was provided to virus-producing cells, the effect of SRP19 overexpression on A3G virion packaging was reversed (Fig. 7). These data demonstrate a role for 7SL RNA in mediating virion packaging of A3G. Overexpression of other A3G-associated cellular factors, such as Ro60 and La, had little effect on A3G virion packaging (Fig. 8).

Diverse retroviruses, such as Rous sarcoma virus (2), murine leukemia virus (16, 33, 34, 52, 55), feline leukemia virus (7), visna virus (36), and HIV-1 (26, 53), have been shown to package Pol III-transcribed RNAs, including 7SL RNA, as well as tRNA primers specific for these various retroviruses. Efficient targeting of A3G into a variety of retroviruses could be mediated by its interaction with virion-associated 7SL RNAs. These interactions would provide an explana-

tion for the broad antiviral activity of A3G against diverse retroviruses. While the NC domain of HIV-1 Gag is required for 7SL RNA packaging, the reason that these RNAs are packaged more efficiently than other abundant cellular RNAs, such as Y RNAs or β-actin mRNA, is not known. Although this possibility is currently only speculative, some of the Pol III RNAs other than primer tRNA may play additional roles during retroviral infection. For example, together with viral genomic RNA, they may act as a scaffold during Gag assembly. Alternatively, certain Pol III RNAs might be more abundant at the site of virus assembly and be packaged passively as a result.

A3G interacted efficiently with certain Pol III RNAs, such as Y3 and 7SL RNAs, but not 5S rRNA. The specificity of the A3G interaction with certain Pol III RNAs cannot be explained by the relative abundance of the various RNAs, since 5S rRNA is also an abundant cytoplasmic RNA in 293/A3G-HA cells (data not shown). Furthermore, although intracellular Y4 and Y5 RNA levels were comparable, the A3G interaction with Y4 RNA was much stronger than that with Y5 RNA (Fig. 2). Interaction of A3G with cellular mRNAs, including A3G mRNA, has been reported (12, 20, 30, 67). However, we found that among A3G-HA-associated RNAs, 7SL RNA was >100-fold more abundant than A3G mRNA or GAPDH mRNA (Fig. 2A). It is conceivable that A3G recognizes certain RNA sequences and/or structures that are shared by particular Y RNAs and 7SL RNA. Selective binding of A3G with Y and 7SL RNAs may also be mediated by an unidentified adaptor molecule(s). However, SRP19 inhibited the interaction of 7SL RNA with A3G but not that of A3G with Y3 RNA (data not shown). More experiments are required to identify the mechanism governing the selective binding of Y and 7SL RNAs by A3G.

Could the association of A3G with Y RNAs and 7SL RNA have any cellular function(s)? It is interesting that A3G interacts with 7SL RNA, which is apparently not part of the SRP complexes. A3G interacts with 7SL RNA but not SRP54 proteins (Fig. 3), suggesting that the binding of one or more SRP proteins to 7SL RNA may interfere with the recognition of 7SL RNA by A3G. The cellular role of 7SL RNAs that are not part of the SRP complexes is not clear. The potential cellular function of 7SL RNA-A3G complexes also requires more investigation. Unlike 7SL RNA and SRP complexes, the interaction of Ro60 with Y RNAs did not prevent A3G binding to Y RNAs, since both Ro60 and Y RNAs were coprecipitated with A3G. Ro60 is thought to contribute to small RNA quality control (11). Whether A3G could participate in Pol III RNA editing or quality control is an intriguing question. Future studies will help to determine whether the interaction of A3G with Y and 7SL RNAs has other as-yet-unidentified cellular function(s) in addition to retroviral restriction.

REFERENCES

1. **Alce, T. M., and W. Popik.** 2004. APOBEC3G is incorporated into virus-like particles by a direct interaction with HIV-1 Gag nucleocapsid protein. J. Biol. Chem. **279:**34083–34086.

1a. **Ausubel, F. M., R. Brent, R. E. Kingston, D. D. Moore, J. G. Seidman, J. A. Smith, and K. Struhl (ed.).** 2003. Current protocols on molecular biology. John Wiley & Sons, Inc., New York, NY.

2. **Bishop, J. M., W. E. Levinson, D. Sullivan, L. Fanshier, N. Quintrell, and J. Jackson.** 1970. The low-molecular-weight RNAs of Rous sarcoma virus. II. 7S RNA. Virology **42:**927–937.

3. **Bishop, K. N., R. K. Holmes, and M. H. Malim.** 2006. Antiviral potency of APOBEC proteins does not correlate with cytidine deamination. J. Virol. **80:**8450–8458.

4. **Bishop, K. N., R. K. Holmes, A. M. Sheehy, N. O. Davidson, S. J. Cho, and M. H. Malim.** 2004. Cytidine deamination of retroviral DNA by diverse APOBEC proteins. Curr. Biol. **14:**1392–1396.

5. **Bogerd, H. P., H. L. Wiegand, B. P. Doehle, K. K. Lueders, and B. R. Cullen.** 2006. APOBEC3A and APOBEC3B are potent inhibitors of LTR-retrotransposon function in human cells. Nucleic Acids Res. **34:**89–95.

6. **Bogerd, H. P., H. L. Wiegand, A. E. Hulme, J. L. Garcia-Perez, K. S. O'Shea, J. V. Moran, and B. R. Cullen.** 2006. Cellular inhibitors of long interspersed element 1 and Alu retrotransposition. Proc. Natl. Acad. Sci. USA **103:**8780–8785.

7. **Brian, D. A., A. R. Thomason, F. M. Rottman, and L. F. Velicer.** 1975. Properties of feline leukemia virus. III. Analysis of the RNA. J. Virol. **16:**535–545.

8. **Burnett, A., and P. Spearman.** 2007. APOBEC3G multimers are recruited to the plasma membrane for packaging into human immunodeficiency virus type 1 virus-like particles in an RNA-dependent process requiring the NC basic linker. J. Virol. **81:**5000–5013.

9. **Cen, S., F. Guo, M. Niu, J. Saadatmand, J. Deflassieux, and L. Kleiman.** 2004. The interaction between HIV-1 Gag and APOBEC3G. J. Biol. Chem. **279:**33177–33184.

10. **Chen, H., C. E. Lilley, Q. Yu, D. V. Lee, J. Chou, I. Narvaiza, N. R. Landau, and M. D. Weitzman.** 2006. APOBEC3A is a potent inhibitor of adeno-associated virus and retrotransposons. Curr. Biol. **16:**480–485.

11. **Chen, X., and S. L. Wolin.** 2004. The Ro 60 kDa autoantigen: insights into cellular function and role in autoimmunity. J. Mol. Med. **82:**232–239.

12. **Chiu, Y. L., H. E. Witkowska, S. C. Hall, M. Santiago, V. B. Soros, C. Esnault, T. Heidmann, and W. C. Greene.** 2006. High-molecular-mass APOBEC3G complexes restrict Alu retrotransposition. Proc. Natl. Acad. Sci. USA **103:**15588–15593.

13. **Conticello, S. G., R. S. Harris, and M. S. Neuberger.** 2003. The Vif protein of HIV triggers degradation of the human antiretroviral DNA deaminase APOBEC3G. Curr. Biol. **13:**2009–2013.

14. **Doehle, B. P., A. Schafer, and B. R. Cullen.** 2005. Human APOBEC3B is a potent inhibitor of HIV-1 infectivity and is resistant to HIV-1 Vif. Virology **339:**281–288.

15. **Douaisi, M., S. Dussart, M. Courcoul, G. Bessou, R. Vigne, and E. Decroly.** 2004. HIV-1 and MLV Gag proteins are sufficient to recruit APOBEC3G into virus-like particles. Biochem. Biophys. Res. Commun. **321:**566–573.

16. **Duesberg, P. H., and W. S. Robinson.** 1966. Nucleic acid and proteins isolated from the Rauscher mouse leukemia virus (MLV). Proc. Natl. Acad. Sci. USA **55:**219–227.

17. **Dutko, J. A., A. Schafer, A. E. Kenny, B. R. Cullen, and M. J. Curcio.** 2005. Inhibition of a yeast LTR retrotransposon by human APOBEC3 cytidine deaminases. Curr. Biol. **15:**661–666.

18. **Egea, P. F., R. M. Stroud, and P. Walter.** 2005. Targeting proteins to membranes: structure of the signal recognition particle. Curr. Opin. Struct. Biol. **15:**213–220.

19. **Esnault, C., O. Heidmann, F. Delebecque, M. Dewannieux, D. Ribet, A. J. Hance, T. Heidmann, and O. Schwartz.** 2005. APOBEC3G cytidine deaminase inhibits retrotransposition of endogenous retroviruses. Nature **433:**430–433.

20. **Gallois-Montbrun, S., B. Kramer, C. M. Swanson, H. Byers, S. Lynham, M. Ward, and M. H. Malim.** 2006. The antiviral protein APOBEC3G localizes to ribonucleoprotein complexes found in P-bodies and stress granules. J. Virol. **81:**2165–2178.

21. **Guo, F., S. Cen, M. Niu, J. Saadatmand, and L. Kleiman.** 2006. Inhibition of formula-primed reverse transcription by human APOBEC3G during human immunodeficiency virus type 1 replication. J. Virol. **80:**11710–11722.

22. **Harris, R. S., K. N. Bishop, A. M. Sheehy, H. M. Craig, S. K. Petersen-Mahrt, I. N. Watt, M. S. Neuberger, and M. H. Malim.** 2003. DNA deamination mediates innate immunity to retroviral infection. Cell **113:**803–809.

23. **Harris, R. S., and M. T. Liddament.** 2004. Retroviral restriction by APOBEC proteins. Nat. Rev. Immunol. **4:**868–877.

24. **Huthoff, H., and M. H. Malim.** 2007. Identification of amino acid residues in APOBEC3G required for regulation by human immunodeficiency virus type 1 Vif and virion encapsidation. J. Virol. **81:**3807–3815.

25. **Jarmuz, A., A. Chester, J. Bayliss, J. Gisbourne, I. Dunham, J. Scott, and N. Navaratnam.** 2002. An anthropoid-specific locus of orphan C to U RNA-editing enzymes on chromosome 22. Genomics **79:**285–296.

26. **Jiang, M., J. Mak, M. A. Wainberg, M. A. Parniak, E. Cohen, and L. Kleiman.** 1992. Variable tRNA content in HIV-1IIIB. Biochem. Biophys. Res. Commun. **185:**1005–1015.

27. **Kaiser, S. M., and M. Emerman.** 2006. Uracil DNA glycosylase is dispensable for human immunodeficiency virus type 1 replication and does not contribute to the antiviral effects of the cytidine deaminase Apobec3G. J. Virol. **80:**875–882.

28. **Khan, M. A., S. Kao, E. Miyagi, H. Takeuchi, R. Goila-Gaur, S. Opi, C. L. Gipson, T. G. Parslow, H. Ly, and K. Strebel.** 2005. Viral RNA is required for the association of APOBEC3G with human immunodeficiency virus type 1 nucleoprotein complexes. J. Virol. **79:**5870–5874.

29. **Kobayashi, M., A. Takaori-Kondo, Y. Miyauchi, K. Iwai, and T. Uchiyama.** 2005. Ubiquitination of APOBEC3G by an HIV-1 Vif-Cullin5-Elongin B-Elongin C complex is essential for Vif function. J. Biol. Chem. **280:**18573–18578.

30. **Kozak, S. L., M. Marin, K. M. Rose, C. Bystrom, and D. Kabat.** 2006. The anti-HIV-1 editing enzyme APOBEC3G binds HIV-1 RNA and messenger RNAs that shuttle between polysomes and stress granules. J. Biol. Chem. **281:**29105–29119.

31. **Langlois, M. A., R. C. Beale, S. G. Conticello, and M. S. Neuberger.** 2005. Mutational comparison of the single-domained APOBEC3C and double-domained APOBEC3F/G anti-retroviral cytidine deaminases provides insight into their DNA target site specificities. Nucleic Acids Res. **33:**1913–1923.

32. **Lecossier, D., F. Bouchonnet, F. Clavel, and A. J. Hance.** 2003. Hypermutation of HIV-1 DNA in the absence of the Vif protein. Science **300:**1112.

33. **Levin, J. G., P. M. Grimley, J. M. Ramseur, and I. K. Berezesky.** 1974. Deficiency of 60 to 70S RNA in murine leukemia virus particles assembled in cells treated with actinomycin D. J. Virol. **14:**152–161.

34. **Levin, J. G., and J. G. Seidman.** 1979. Selective packaging of host tRNA's by murine leukemia virus particles does not require genomic RNA. J. Virol. **29:**328–335.

35. **Liddament, M. T., W. L. Brown, A. J. Schumacher, and R. S. Harris.** 2004. APOBEC3F properties and hypermutation preferences indicate activity against HIV-1 in vivo. Curr. Biol. **14:**1385–1391.

36. **Lin, F. H., and H. Thormar.** 1971. Characterization of ribonucleic acid from visna virus. J. Virol. **7:**582–587.

37. **Liu, B., P. T. Sarkis, K. Luo, Y. Yu, and X. F. Yu.** 2005. Regulation of Apobec3F and human immunodeficiency virus type 1 Vif by Vif-Cul5-ElonB/C E3 ubiquitin ligase. J. Virol. **79:**9579–9587.

38. **Liu, B., X. Yu, K. Luo, Y. Yu, and X. F. Yu.** 2004. Influence of primate lentiviral Vif and proteasome inhibitors on human immunodeficiency virus type 1 virion packaging of APOBEC3G. J. Virol. **78:**2072–2081.

39. **Luo, K., B. Liu, Z. Xiao, Y. Yu, X. Yu, R. Gorelick, and X. F. Yu.** 2004. Amino-terminal region of the human immunodeficiency virus type 1 nucleocapsid is required for human APOBEC3G packaging. J. Virol. **78:**11841–11852.

40. **Luo, K., T. Wang, B. Liu, C. Tian, Z. Xiao, J. Kappes, and X.-F. Yu.** 2007. Cytidine deaminases APOBEC3G and APOBEC3F interact with human immunodeficiency virus type 1 integrase and inhibit proviral DNA formation. J. Virol. **81:**7238–7248.

41. **Luo, K., Z. Xiao, E. Ehrlich, Y. Yu, B. Liu, S. Zheng, and X. F. Yu.** 2005. Primate lentiviral virion infectivity factors are substrate receptors that assemble with cullin 5-E3 ligase through a HCCH motif to suppress APOBEC3G. Proc. Natl. Acad. Sci. USA **102:**11444–11449.

42. **Mangeat, B., P. Turelli, G. Caron, M. Friedli, L. Perrin, and D. Trono.** 2003. Broad antiretroviral defense by human APOBEC3G through lethal editing of nascent reverse transcripts. Nature **424:**99–103.

43. **Mariani, R., D. Chen, B. Schrofelbauer, F. Navarro, R. Konig, B. Bollman, C. Munk, H. Nymark-McMahon, and N. R. Landau.** 2003. Species-specific exclusion of APOBEC3G from HIV-1 virions by Vif. Cell **114:**21–31.

44. **Marin, M., K. M. Rose, S. L. Kozak, and D. Kabat.** 2003. HIV-1 Vif protein binds the editing enzyme APOBEC3G and induces its degradation. Nat. Med. **9:**1398–1403.

45. **Mbisa, J. L., R. Barr, J. A. Thomas, N. Vandegraaff, I. J. Dorweiler, E. S. Svarovskaia, W. L. Brown, L. M. Mansky, R. J. Gorelick, R. S. Harris, A. Engelman, and V. K. Pathak.** 2007. Human immunodeficiency virus type 1 cDNAs produc1ed in the presence of APOBEC3G exhibit defects in plus-strand DNA transfer and integration. J. Virol. **81:**7099–7110.

46. **Mehle, A., J. Goncalves, M. Santa-Marta, M. McPike, and D. Gabuzda.** 2004. Phosphorylation of a novel SOCS-box regulates assembly of the HIV-1 Vif-Cul5 complex that promotes APOBEC3G degradation. Genes Dev. **18:**2861–2866.

47. **Mehle, A., E. R. Thomas, K. S. Rajendran, and D. Gabuzda.** 2006. A zinc-binding region in Vif binds Cul5 and determines cullin selection. J. Biol. Chem. **281:**17259–17265.

48. **Menichelli, E., C. Isel, C. Oubridge, and K. Nagai.** 2007. Protein-induced conformational changes of RNA during the assembly of human signal recognition particle. J. Mol. Biol. **367:**187–203.

49. **Misra, S., M. K. Tripathi, and G. Chaudhuri.** 2005. Down-regulation of 7SL

RNA expression and impairment of vesicular protein transport pathways by Leishmania infection of macrophages. J. Biol. Chem. **280:**29364–29373.

50. **Muckenfuss, H., M. Hamdorf, U. Held, M. Perkovic, J. Lower, K. Cichutek, E. Flory, G. G. Schumann, and C. Munk.** 2006. APOBEC3 proteins inhibit human LINE-1 retrotransposition. J. Biol. Chem. **281:**22161–22172.

51. **Navarro, F., B. Bollman, H. Chen, R. Konig, Q. Yu, K. Chiles, and N. R. Landau.** 2005. Complementary function of the two catalytic domains of APOBEC3G. Virology **333:**374–386.

52. **Onafuwa-Nuga, A. A., S. R. King, and A. Telesnitsky.** 2005. Nonrandom packaging of host RNAs in Moloney murine leukemia virus. J. Virol. **79:**13528–13537.

53. **Onafuwa-Nuga, A. A., A. Telesnitsky, and S. R. King.** 2006. 7SL RNA, but not the 54-kd signal recognition particle protein, is an abundant component of both infectious HIV-1 and minimal virus-like particles. RNA **12:**542–546.

54. **Oubridge, C., A. Kuglstatter, L. Jovine, and K. Nagai.** 2002. Crystal structure of SRP19 in complex with the S domain of SRP RNA and its implication for the assembly of the signal recognition particle. Mol. Cell **9:**1251–1261.

55. **Peters, G., F. Harada, J. E. Dahlberg, A. Panet, W. A. Haseltine, and D. Baltimore.** 1977. Low-molecular-weight RNAs of Moloney murine leukemia virus: identification of the primer for RNA-directed DNA synthesis. J. Virol. **21:**1031–1041.

56. **Schafer, A., H. P. Bogerd, and B. R. Cullen.** 2004. Specific packaging of APOBEC3G into HIV-1 virions is mediated by the nucleocapsid domain of the gag polyprotein precursor. Virology **328:**163–168.

57. **Schrofelbauer, B., Q. Yu, S. G. Zeitlin, and N. R. Landau.** 2005. Human immunodeficiency virus type 1 Vpr induces the degradation of the UNG and SMUG uracil-DNA glycosylases. J. Virol. **79:**10978–10987.

58. **Schumacher, A. J., D. V. Nissley, and R. S. Harris.** 2005. APOBEC3G hypermutates genomic DNA and inhibits Ty1 retrotransposition in yeast. Proc. Natl. Acad. Sci. USA **102:**9854–9859.

59. **Sheehy, A. M., N. C. Gaddis, J. D. Choi, and M. H. Malim.** 2002. Isolation of a human gene that inhibits HIV-1 infection and is suppressed by the viral Vif protein. Nature **418:**646–650.

60. **Sheehy, A. M., N. C. Gaddis, and M. H. Malim.** 2003. The antiretroviral enzyme APOBEC3G is degraded by the proteasome in response to HIV-1 Vif. Nat. Med. **9:**1404–1407.

61. **Stenglein, M. D., and R. S. Harris.** 2006. APOBEC3B and APOBEC3F inhibit L1 retrotransposition by a DNA deamination-independent mechanism. J. Biol. Chem. **281:**16837–16841.

62. **Stopak, K., C. de Noronha, W. Yonemoto, and W. C. Greene.** 2003. HIV-1 Vif blocks the antiviral activity of APOBEC3G by impairing both its translation and intracellular stability. Mol. Cell **12:**591–601.

63. **Suspene, R., P. Sommer, M. Henry, S. Ferris, D. Guetard, S. Pochet, A. Chester, N. Navaratnam, S. Wain-Hobson, and J. P. Vartanian.** 2004. APOBEC3G is a single-stranded DNA cytidine deaminase and functions independently of HIV reverse transcriptase. Nucleic Acids Res. **32:**2421–2429.

64. **Svarovskaia, E. S., H. Xu, J. L. Mbisa, R. Barr, R. J. Gorelick, A. Ono, E. O. Freed, W. S. Hu, and V. K. Pathak.** 2004. Human apolipoprotein B mRNA-editing enzyme-catalytic polypeptide-like 3G (APOBEC3G) is incorporated into HIV-1 virions through interactions with viral and nonviral RNAs. J. Biol. Chem. **279:**35822–35828.

65. **Turelli, P., B. Mangeat, S. Jost, S. Vianin, and D. Trono.** 2004. Inhibition of hepatitis B virus replication by APOBEC3G. Science **303:**1829.

66. **Turelli, P., and D. Trono.** 2005. Editing at the crossroad of innate and adaptive immunity. Science **307:**1061–1065.

67. **Wichroski, M. J., G. B. Robb, and T. M. Rana.** 2006. Human retroviral host restriction factors APOBEC3G and APOBEC3F localize to mRNA processing bodies. PLoS Pathog. **2:**e41.

68. **Wiegand, H. L., B. P. Doehle, H. P. Bogerd, and B. R. Cullen.** 2004. A second human antiretroviral factor, APOBEC3F, is suppressed by the HIV-1 and HIV-2 Vif proteins. EMBO J. **23:**2451–2458.

69. **Xiao, Z., E. Ehrlich, K. Luo, Y. Xiong, and X. F. Yu.** 2007. Zinc chelation inhibits HIV Vif activity and liberates antiviral function of the cytidine deaminase APOBEC3G. FASEB J. **21:**217–222.

70. **Xiao, Z., E. Ehrlich, Y. Yu, K. Luo, T. Wang, C. Tian, and X. F. Yu.** 2006. Assembly of HIV-1 Vif-Cul5 E3 ubiquitin ligase through a novel zinc-binding domain-stabilized hydrophobic interface in Vif. Virology **349:**290–299.

71. **Yang, B., K. Chen, C. Zhang, S. Huang, and H. Zhang.** 2007. Virion-associated Uracil DNA glycosylase-2 and apurinic/apyrimidinic endonuclease are involved in the degradation of APOBEC3G-edited nascent HIV-1 DNA. J. Biol. Chem. **282:**11667–11675.

72. **Yu, Q., D. Chen, R. Konig, R. Mariani, D. Unutmaz, and N. R. Landau.** 2004. APOBEC3B and APOBEC3C are potent inhibitors of simian immunodeficiency virus replication. J. Biol. Chem. **279:**53379–53386.

73. **Yu, Q., R. Konig, S. Pillai, K. Chiles, M. Kearney, S. Palmer, D. Richman, J. M. Coffin, and N. R. Landau.** 2004. Single-strand specificity of APOBEC3G accounts for minus-strand deamination of the HIV genome. Nat. Struct. Mol. Biol. **11:**435–442.

74. **Yu, X., Y. Yu, B. Liu, K. Luo, W. Kong, P. Mao, and X. F. Yu.** 2003. Induction of APOBEC3G ubiquitination and degradation by an HIV-1 Vif-Cul5-SCF complex. Science **302:**1056–1060.

75. **Yu, Y., Z. Xiao, E. S. Ehrlich, X. Yu, and X. F. Yu.** 2004. Selective assembly of HIV-1 Vif-Cul5-ElonginB-ElonginC E3 ubiquitin ligase complex through a novel SOCS box and upstream cysteines. Genes Dev. **18:**2867–2872.

76. **Zennou, V., D. Perez-Caballero, H. Gottlinger, and P. D. Bieniasz.** 2004. APOBEC3G incorporation into human immunodeficiency virus type 1 particles. J. Virol. **78:**12058–12061.

77. **Zhang, H., B. Yang, R. J. Pomerantz, C. Zhang, S. C. Arunachalam, and L. Gao.** 2003. The cytidine deaminase CEM15 induces hypermutation in newly synthesized HIV-1 DNA. Nature **424:**94–98.

78. **Zhang, K. L., B. Mangeat, M. Ortiz, V. Zoete, D. Trono, A. Telenti, and O. Michielin.** 2007. Model structure of human APOBEC3G. PLoS ONE. **2:**e378.

79. **Zheng, Y. H., D. Irwin, T. Kurosu, K. Tokunaga, T. Sata, and B. M. Peterlin.** 2004. Human APOBEC3F is another host factor that blocks human immunodeficiency virus type 1 replication. J. Virol. **78:**6073–6076.